INTERNATIONAL JOURNAL OF CLIMATOLOGY
Int. J. Climatol. (2016)
Published online in Wiley Online Library
(wileyonlinelibrary.com) DOI: 10.1002/joc.4757

RMetS
Royal Meteorological Society

Analysis of waterspout environmental conditions and of parent-storm behaviour based on satellite data over the southern Aegean Sea of Greece

I. T. Matsangouras,[a,b]* P. T. Nastos,[a] H. B. Bluestein,[c] I. Pytharoulis,[d] K. Papachristopoulou[a] and M. M. Miglietta[e]

[a] *Laboratory of Climatology and Atmospheric Environment, Faculty of Geology and Geoenvironment, Department of Geography and Climatology, University of Athens, Greece*
[b] *Hellenic National Meteorological Service, Athens, Greece*
[c] *School of Meteorology, University of Oklahoma, Norman, OK, USA*
[d] *Department of Meteorology and Climatology, School of Geology, Aristotle University of Thessaloniki, Greece*
[e] *Institute of Atmospheric Sciences and Climate, Italian National Research Council, Lecce, Italy*

ABSTRACT: A frequent area of waterspout formation is identified over the southern Aegean Sea. The objectives of this study are threefold: (1) to investigate the temporal evolution of Cloud Top Temperature (CTT) of cloud lines (waterspouts' parent clouds) that triggered the formation of single or multiple waterspout events, by using Meteorological Satellite Second Generation infrared satellite data, cloud base height data and weather observations from the closest Hellenic National Meteorological Service meteorological station; (2) to synthesize a detailed climatology of the thermodynamic environment during waterspout activity and (3) to explore the sea-surface temperature (SST) seasonal distribution and its possible relationships with the temperature of the middle and lower troposphere during waterspout days over the southern Aegean Sea.

It was found that the CTT of waterspout parent clouds decreases close to waterspout formation time, which is consistent with growing clouds. The Severe Weather Threat Index (SWEAT), the Bulk Richardson Number (BRN) and the Convective Potential Available Energy during the autumn season were consistent with a shallow-convection environment. The instability parameter ΔT^{1000} (difference in the air temperature between 1000 hPa and that at other pressure levels) exhibited a symmetric distribution about the median during both seasons and at all levels. More than 75% of autumn waterspout activity over the southern Aegean Sea developed with SST values varying from 22 to 24.5 °C, while the instability parameter ΔT^{SST} (the temperature difference between the SST and the temperature at various pressure levels) exhibited a symmetrical distribution about the median for both seasons and for all pressure levels, consistent with the ΔT^{1000} seasonal distribution. A statistical analysis showed that the means of SWEAT, BRN, convective inhibition, SST, ΔT^{SST} and ΔT^{1000} from air temperature at 700 hPa differ statistically significant ($p < 0.001$) between waterspout and non-waterspout days in autumn, over the southern Aegean Sea, during 2005–2012.

KEY WORDS waterspouts; remote sensing; satellite; MSG; SEVIRI; SST; brightness temperature; soundings; thermodynamic indices; instability; Aegean Sea

Received 18 June 2015; Revised 25 March 2016; Accepted 30 March 2016

1. Introduction

Although waterspouts are overall less intense than their tornadic counterparts over land, there are several cases in which waterspouts were hazardous, having the ability to produce significant loss of both property and life. The primary risk from waterspouts concerns residents, mariners and structures in coastal areas and large inland lakes. An increasing interest in the detection of these phenomena has emerged in the Mediterranean in the last few years (Gianfreda *et al.*, 2005; Giaiotti *et al.*, 2007; Gaya, 2011; Miglietta and Rotunno, 2016). Matsangouras *et al.* (2014) documented the impact of tornadoes and waterspouts over Greece based on historic (1795–1999) and recent data sets (2000–2012) of waterspout and tornado events. A remarkable event occurred at Megdova Lake of Karditsa (central Greece) during the morning of 17 December 1959, when a lethal waterspout destroyed the boat of 21 workers (Matsangouras *et al.*, 2014).

The characteristics of waterspouts have been described in detail by Golden (1968, 1971, 1973, 1974a, 1974b, 1977), Leverson *et al.* (1977), Simpson *et al.* (1986), Golden and Sabones (1991), Golden and Bluestein (1993), Wakimoto and Lew (1993), Rennó and Bluestein (2001) and Golden (2003). Fundamental processes of waterspout formation and the identification of the water-surface

* Correspondence to: I. T. Matsangouras, Laboratory of Climatology and Atmospheric Environment, Faculty of Geology and Geoenvironment, Department of Geography and Climatology, University of Athens, University Campus, Zografou, 15784 Athens, Greece. E-mail: john_matsa@geol.uoa.gr

signatures of waterspouts in relation to their development stage and intensity were described by Golden (1973, 1974a, 1974b, 1977, 2003) in which the following five stages of waterspout were identified: (1) the dark spot, (2) the spiral pattern, (3) the spray ring, (4) the mature waterspout and (5) the decay stage. Waterspouts rotate either cyclonically or anticyclonically (Golden, 1974a; Schwiesow, 1981), having surface diameters between 5 and 75 m; they receive their vorticity from local horizontal wind shear. The air temperature and pressure perturbations observed within waterspouts vary from 0.2 to 2.5 K and from 10 to 90 hPa (Golden, 1974a; Leverson *et al.*, 1977), respectively. Rennó and Bluestein (2001) showed that the scaling theory for dust devils proposed by Rennó *et al.* (1998) is also successful in predicting the intensity of waterspouts. Waterspouts usually form under convective clouds (Golden, 1974a). Regions of local horizontal shear lines, separating the updrafts from downdrafts, are favoured for waterspout genesis (Golden, 1974a; Hess and Spillane, 1990), although this condition is a necessary but not a sufficient condition for waterspout formation (Simpson *et al.*, 1986). Perhaps from the different surface friction, from a dynamic point of view, waterspouts and tornadoes are similar (Bluestein, 2013). Depending on the mesocyclone or non-mesocyclone nature, respectively, large or weak vertical wind shear is needed in environment conducive to their formation (Markowski and Richardson, 2010).

In contrast to the US tornado database, *Storm Data* (Schaefer and Edwards, 1999; McCarthy, 2003), which is co-maintained by the National Climatic Data Center (http://www.ncdc.noaa.gov) and the Storm Prediction Center (http://www.spc.noaa.gov), several researchers at the European Severe Storms Laboratory (ESSL) have put considerable effort in developing a tornado and waterspout database in Europe for their respective home countries, resulting in an open database, the European Severe Weather Database (Dotzek *et al.*, 2009). A similar effort has been followed by the Laboratory of Climatology and Atmospheric Environment (LACAE, http://lacae.geol.uoa.gr) at the University of Athens, in order to record tornadoes and waterspouts in Greece and over the eastern Mediterranean (Matsangouras and Nastos, 2014). LACAE is collaborating closely with ESSL, to overcome the strong underreporting in the Mediterranean region and Eastern Europe (Groenemeijer and Kühne, 2014). Indeed, LACAE in 2009 developed an open-ended, online tornado reporting system (http://tornado.geol.uoa.gr), contributing to the compilation of a climatology and numerical analysis of these extreme weather events (Matsangouras *et al.*, 2014, 2016). Based on this database, an updated climatology of waterspouts and tornadoes was presented by Matsangouras *et al.* (2014), corroborating previous climatological studies by Nastos and Matsangouras (2010) and Sioutas (2011) regarding spatial and temporal tornadic activity during the 20th century and 2000–2009, respectively. Moreover, Matsangouras *et al.* (2014) highlighted specific seasonal patterns (e.g. tornadoes over NW Peloponnese during autumn and waterspouts over the southern Aegean Sea during autumn and winter).

In recent decades, remote-sensing data (satellite or radar images) have enhanced research efforts by providing an unprecedented amount of data for significant atmospheric variables in regions with sparse surface coverage of temperature, wind, etc. In this study, Cloud Top Temperature (hereafter, CTT) derived from the Spinning Enhanced Visible and InfraRed Imager (SEVIRI) of European Organisation for the Exploitation of Meteorological Satellites (EUMETSAT) Meteorological Satellite Second Generation (MSG) was used to investigate the evolution of parent waterspout clouds over the southern Aegean Sea. The CTT data were obtained from the infrared (hereafter, IR) spectrum (Channel 9, 10.8 μm) and used as an essential tool in detecting cloud tops and measuring the cloud-top brightness temperature (hereafter, BT).

The goal of this study is to analyse a recent data set documenting waterspout activity over the southern Aegean Sea, using updated weather satellite products depicting the CTT of the waterspout parent cloud, combined with upper air and surface-observation data from the nearest meteorological station. More specifically, the objectives of our research are: (1) to synthesize and analyse a detailed climatology of the thermodynamic environment; (2) to investigate the evolution of the waterspout parent cloud during a specific time window, from 1 h prior to until 1 h after waterspout time formation, by using the CTT product of the MSG SEVIRI instrument and (3) to explore the sea-surface temperature (hereafter, SST) seasonal distribution and its possible relationships with the temperature of the middle and lower troposphere, during waterspout days over the southern Aegean Sea. This study contributes to a better awareness of the operational forecasters, so that to evaluate the atmospheric conditions that favour waterspouts, taking into account the presented climatology of the thermodynamic environment over the southern Aegean Sea.

The outline of the paper is as follows: Section 2 identifies the data sources and the methodology adopted. Results and discussion are given in Sections 3 and 4, respectively. Finally, Section 5 summarizes our findings and conclusions.

2. Data and methodology

2.1. The LACAE waterspout database

The domain of our climatology and analysis is the southern Aegean Sea (Figure 1), or more specifically, the sea area north of Heraklion (D12 in Matsangouras *et al.*, 2014). This area has experienced a mean annual number of eight waterspout events based on 2000–2012 LACAE's database; autumn is the dominant season followed by winter (Matsangouras *et al.*, 2014). Waterspouts over the southern Aegean Sea mainly developed close to the north coasts of Crete island. They developed under cumulus line and propagated towards the coast where the decay process takes place. However, there are a few cases that

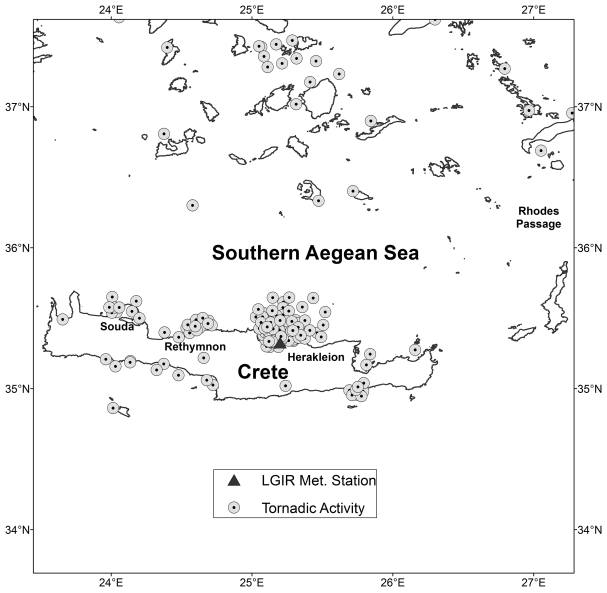

Figure 1. Spatial distribution of tornadic activity over the southern Aegean Sea, within 2005–2012 period, derived from LACAE's database.

documented waterspouts moved into the mainland and decayed a few minutes later, causing significant damages to the local society. Their lifetime is characterized with a short living period (1–5 min); however, there were several cases where multiple waterspouts events developed in a short time window (10–90 min). Figure 2(a) and (b) illustrates the spray ring and mature stage of a typically waterspout event that developed close to Heraklion City coast on 12 October 2012. The mature and decay stage of a multiple waterspout event that took place at Heraklion coast on 6 January 2015 are illustrated in Figure 2(c) and (d), respectively.

Reports of single or multiple waterspout and funnel-cloud events (over water body) were extracted from LACAE's online tornado report database. Funnel cloud reports over the water body were categorized as waterspout events, as the vortex over the water represents the second stage of the waterspout life cycle (Golden, 1974a, 1977). The study period begins with the operational availability of CTT product on 19 January 2004 and ends on 14 November 2013. The first waterspout event occurred on 8 March 2005 and the last one on 14 November 2013. A waterspout day is defined as a day with at least one waterspout; thus, from 2005 to 2013, 110 waterspout events were recorded in LACAE's database on 26 waterspout days (as there were days with multiple waterspout events). There were 11 waterspout days during autumn, 9 days during winter, 5 and 1 during spring and summer, respectively. LACAE's database provided detailed information about the time and the reported location of waterspout occurrence, based on the Google maps interface reporting system (latitude and longitude values), which are essential for the methodology that was followed. When multiple waterspout events occurred during a single day, they were categorized as a single event because they developed over the same area within <90 min under the same parent cloud (e.g. on 21 September 2006, more than 25 waterspouts developed within 90 min over the same area). Thus, a complete data set of 85 waterspout entries out of 110 was available with detailed information about time and latitude/longitude coordinates. This complete waterspout dataset is available at LACAE's database website (http://tornado.geol.uoa.gr/ in database menu). The reader may see Matsangouras *et al.* (2014) and Matsangouras and Nastos (2014) for details about shortcomings in the database.

2.2. SST, upper air and thermodynamic instability data

A daily, high-resolution, real-time, global, SST analysis for the southern Aegean Sea, with a spatial operational grid analysis of 1/12°, was used. This SST analysis was developed by the National Centers for Environmental Prediction/Marine Modeling and Analysis Branch (NCEP/MMAB) and implemented in the NCEP parallel production suite on 16 August 2005, becoming fully operational on 27 September 2005 (http://polar.ncep.noaa.gov/sst/rtg_high_res). Therefore, for the SST analysis, we considered waterspout events that developed between 27 September 2005 and 31 December 2012.

Although the upper-air network of the Hellenic National Meteorological Service (HNMS) is sparse, consisting of only three stations (Thessaloniki in northern, Athens in central and Heraklion in southern Greece), our study area is nearest to the Heraklion (WMO ID: 16754) upper-air meteorological station. Rawinsonde data were retrieved from the University of Wyoming online sounding archive system (http://weather.uwyo.edu/upperair/sounding.html) in order to examine the vertical profile of the lower troposphere. Atmospheric variables (e.g. wind direction and speed, and air temperature) were acquired for the following pressure levels: 500, 700, 850, 925 and 1000 hPa. In addition, the following parameters were employed to summarize the unstable conditions during waterspout days: Convective Potential Available Energy (CAPE), Bulk Richardson Number (BRN), Lifted Index (LI), Showalter Index (SI), K-index (K), Vertical Total (VT), Cross Total (CT), Total Total (TT), Severe Weather Threat (SWEAT) and convective inhibition (CIN). All aforementioned thermodynamic indices are described with references in Table 1. As discussed in Section 1, vertical wind shear is also important. Although not explicitly included among the instability indices, it is implicitly considered here through SWEAT, which includes in its definition the change of wind direction with height and the wind speed in the low-mid troposphere.

2.3. The MSG CTT remote sensing data

CTT remote sensing data for all waterspout events were obtained from the IR 10.8 μm spectra channel (Channel 9) of the MSG SEVIRI radiometer (positioned at 0°). The SEVIRI instrument generates a full-disc image of the earth every 15 min; thus, the CTT products were acquired for every waterspout event for a 2-h period

Figure 2. Photos of a typical waterspout and multiple waterspout events close to the coasts of Heraklion City. The ring spring (a) and mature stage (b) of a waterspout on 12 October 2012. The mature (c) and decay (d) stage of multiple waterspout event on 6 January 2015.

Table 1. Thermodynamic indices used in the study. In the formulae, T denotes air temperature (°C) and D denotes dew point (°C), with one subscript indicating the pressure level (hPa), α denotes the specific volume and another subscript lp denotes a value associated with a lifted parcel; LFC stands for the level of free convection and EL stands for equilibrium level. For the Lifted Index, the lifted parcel concerns a surface parcel with forecast properties at a representative time of day. For the Bulk Richardson Number, $\bar{U}$ denotes the density-weighted speed of the mean vector wind in the layer 0–6 km and U_0 denotes the speed of the mean vector wind in the layer from the surface to 500 m, the quantity $(\bar{U}-U_0)$ is sometimes referred to as the 'BRN shear'.

Index name	Formula	Reference
CAPE (J kg^{-1})	$\mathrm{CAPE} = \int_{\mathrm{LFC}}^{\mathrm{EL}} \left(\alpha_{\mathrm{lp}} - \alpha\right) dp$	Moncrieff and Miller (1976), Glickman (2000)
BRN	$\mathrm{BRN} = \frac{\mathrm{CAPE}}{\frac{1}{2}\left(\overline{U}-U_0\right)^2}$	Weisman and Klemp (1982)
LI (°C)	$\mathrm{LI} = T_{\mathrm{lp}} - T_{500}$	Galway (1956)
SI (°C)	$\mathrm{SI} = T_{500} - T_{\mathrm{lp(850hPa)}}$	Showalter (1947)
K-index (°C)	$K = (T_{850} - T_{500}) + D_{850} - (T_{700} - D_{700})$	George (1960)
VT (°C)	$\mathrm{VT} = T_{850} - T_{500}$	Miller (1967)
CT (°C)	$\mathrm{CT} = D_{850} - T_{500}$	Miller (1967)
TT (°C)	$\mathrm{TT} = \mathrm{VT} + \mathrm{CT}$	Miller (1967)
CIN (J kg^{-1})	$\mathrm{CIN} = \int_{\mathrm{SFC}}^{\mathrm{LFC}} \left(\alpha - \alpha_{\mathrm{lp}}\right) dp$	Williams and Renno (1993)
SWEAT	$\mathrm{SWEAT} = 20(\mathrm{TT}-49°\mathrm{C}) + 12D_{850} + 2V_{850} + V_{500} + 125[\sin(\Delta V500 - 850) + 0.2]$	Miller (1967), Miller *et al.* (1971)

(from 60 min prior to until 60 min after waterspout formation). The spatial resolution of the IR 10.8 µm channel is 3 × 3 km at the sub-satellite point and reduced in our study area to ∼4 km in the E–W direction, and to ∼5 km in the N–S direction. More details about CTT data, format, binary representation, geolocation and conversions of SEVIRI radiances to equivalent temperature can be obtained at EUMETSAT's SEVIRI website (http://www.eumetsat.int).

For every 15-min scan, CTT for the parent cloud was calculated for two specific radii: (1) 5 km (hereafter, R_1) and (2) 10 km (hereafter, R_2). The selection of these radii

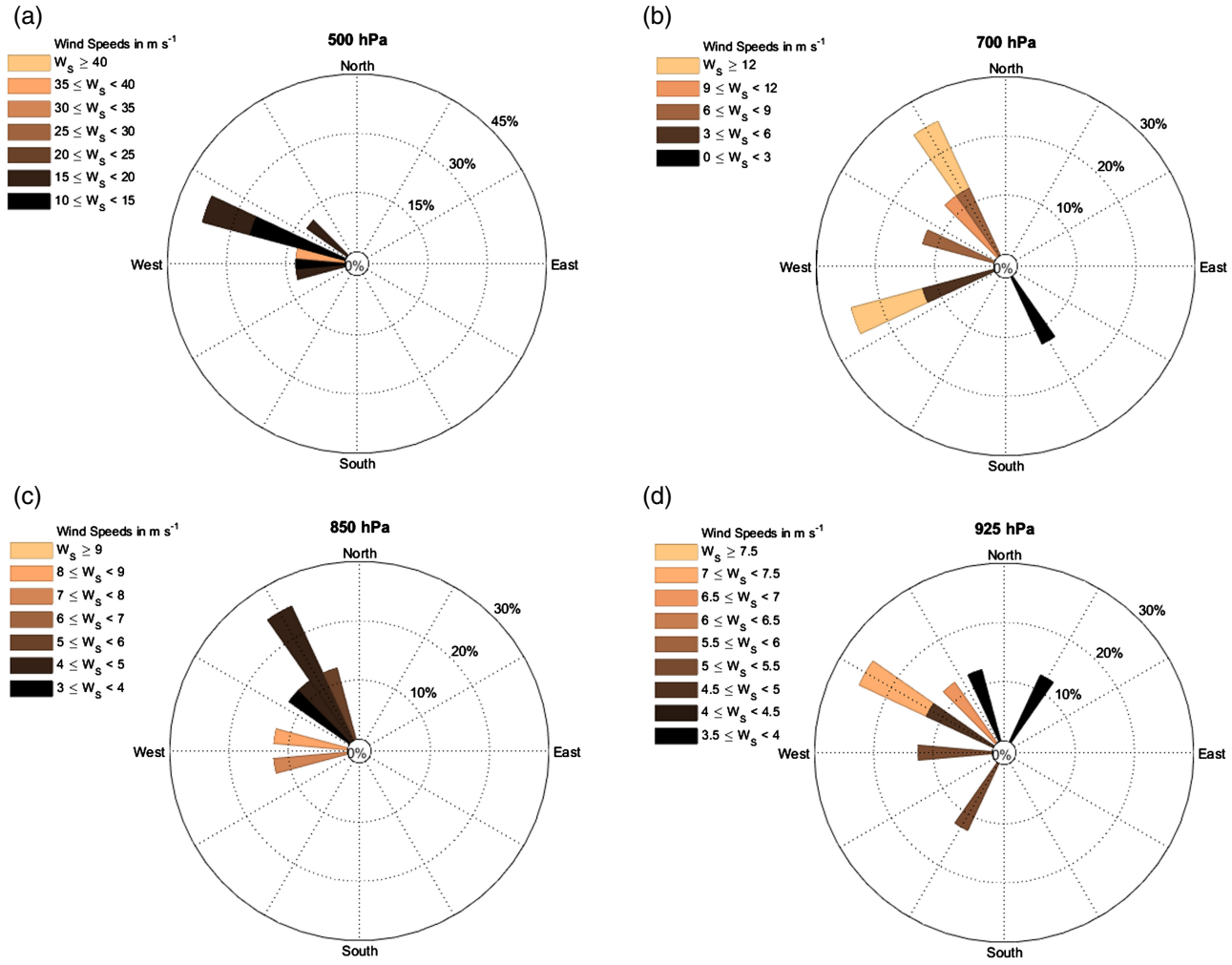

Figure 3. Wind rose graphs (a–d), illustrating the frequency (%) distribution of wind speed ($m\,s^{-1}$) and wind direction (one tenths of a degree), during autumn waterspout days (2005–2012) over the southern Aegean Sea, at the following pressure levels of 500 hPa (a), 700 hPa (b), 850 hPa (c) and 925 hPa (d). Upper air data, during autumn waterspout days, were based on upper air soundings data from HNMS Heraklion meteorological station (WMO ID: 16754).

is based on the CTT pixel spatial resolution, the parallax effect and the spatial scale of the phenomenon. In particular, waterspout parent clouds vary from 2 to 10 km in diameter (Golden, 1974b). The parallax effect is a typical geometric effect associated with satellite measurements. The closer the satellite is to the Earth, the larger the parallax. Thus, this effect is considerable when we observe high clouds or when the clouds are far from the satellite nadir. The parallax at 6.000 m over the study area, based on EUMETSAT's tables, for the northernmost waterspout event was estimated to be 4.5 km to the SE–S (x-axis: 1.6 km and y-axis: 1.6 km) and for the southernmost waterspout event at 4.4 km to the SE–S (x-axis: 1.5 km and y-axis: 4.2 km). These parallax values and the CTT pixel spatial resolution were taken into account to select when the search radius was 5 km or higher. In addition, in this study, we examined the CTT evolution of the parent cloud and not necessarily the CTT at the exact waterspout location. Finally, the cloud base height (CBH) analysis was based on actual aerodrome routine meteorological reports (METAR) from Heraklion (Figure 1) meteorological station (the closest of HNMS meteorological stations). The time series of METARs are available every 30 min and include CBH and cloudiness.

3. Results

3.1. Seasonal analysis of wind, thermodynamic and SST data during waterspout days, 2005–2012

At Heraklion, during autumn waterspout days, at 500 hPa (Figure 3(a)), the dominant wind direction is from the NW. In particular, winds blowing from 300° were observed in more than 40% of the autumn waterspout cases while the wind speed varied from 10 to 20 $m\,s^{-1}$. At 700 hPa (Figure 3(b)), the majority of waterspout events occurred under the influence of northwesterly and west-southwesterly winds while the wind speed did not exceed 15 $m\,s^{-1}$. Wind speed at the lower pressure levels of 850 hPa (Figure 3(c)) and 925 hPa (Figure 3(d)) did not exceed 9 $m\,s^{-1}$. At 850 hPa, the wind direction was mainly from the west or northwest. At 925 hPa, waterspouts

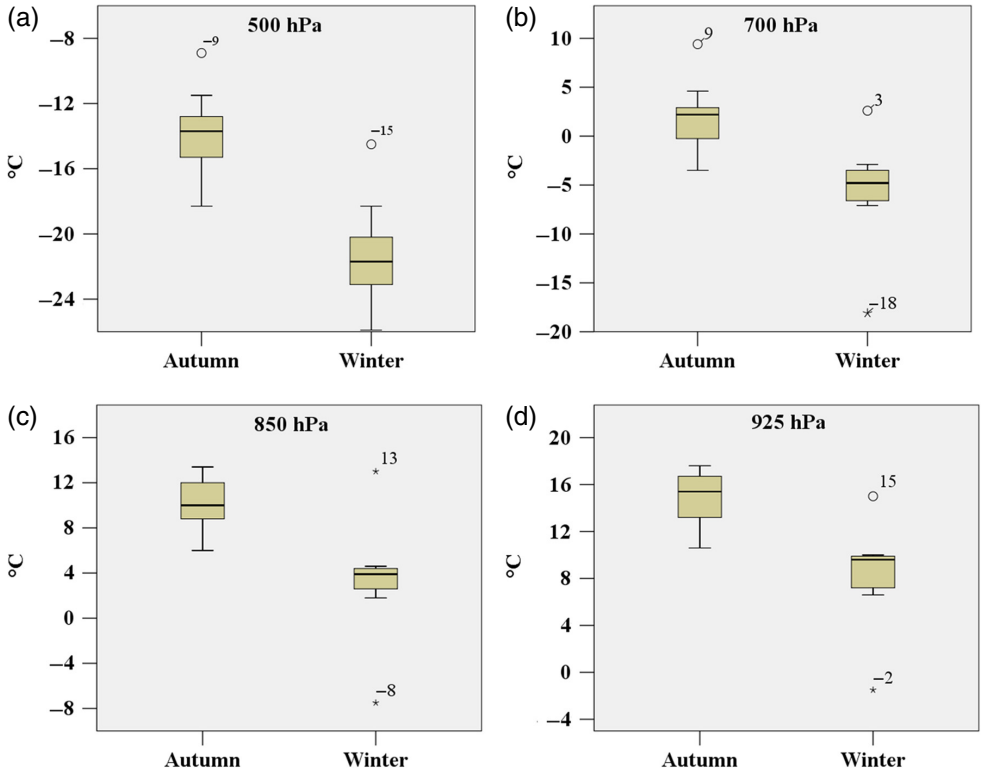

Figure 4. Box-and-whisker plots (a–d) of temperature distribution (°C), during autumn (left variable) and winter (right variable) waterspout days, at 500 hPa (a), 700 hPa (b), 850 hPa (c) and 925 hPa (d) hPa over the southern Aegean Sea. In each box, the central mark (black line) is the median, the edges of the box are the 25th and the 75th percentiles, while the whiskers extended to the most extreme data points and outliers are plotted individually (asterisks or circles). Upper air data, during waterspout days, were based on upper air soundings from HNMS Heraklion meteorological station (WMO ID: 16754).

formed under the influence of NW winds; however, there were a few cases in which the winds blew from the S–SW. At 1000 hPa (not shown), the winds were mainly from 330° at speeds of $<6\,m\,s^{-1}$.

During winter waterspout days (not shown), at 500 hPa, the prevailing wind direction was from the W–NW. At 700 hPa, waterspouts occurred under the influence of winds mainly from the W–SW and NW, while their speeds varied from 8 to 15 and 3 to $10\,m\,s^{-1}$, respectively. At 850 hPa (925 hPa), winds were mainly from the NW (W–NW) at speeds of $<5\,m\,s^{-1}$ ($5–7\,m\,s^{-1}$). At 1000 hPa, the wind distribution was similar to that at 925 hPa, but higher wind speeds were observed from the NW.

Autumn and winter temperature (°C) variability at specific pressure levels during waterspout days are presented in Figure 4 using box-and-whisker plots (autumn: left variable, winter: right variable). At 500 hPa, during autumn waterspouts days (Figure 4(a), left variable), the air temperature varied from −18.3 to −8.4 °C, while lower temperatures were observed during winter, ranging from −25.9 to −14.9 °C (Figure 4(a), right variable). During autumn, the air temperature at 700 hPa varied from −3.5 to 9.4 °C, with the median at 3 °C, against −18.1 to 2.6 °C in winter (Figure 4(b)). It is seen in Figure 4(c) and (d) that at 850 hPa (925 hPa), the air temperature ranged from 6 to 13.4 °C (10.6 to 17.6 °C) during autumn waterspout days, as contrasted with a cooler −7.5 to 13 °C (−1.5 to 15 °C) in winter.

The algebraic difference between the temperature of an air parcel, lifted adiabatically from 850 to 500 hPa, and the environmental temperature at 500 hPa represents the SI (see Table 1). A negative SI indicates an environment in which convection can occur; it is especially useful when there is a shallow cool air mass below 850 hPa concealing greater convective potential aloft. However, the SI only assesses instability in one level of the troposphere and underestimates the convective potential for cool layers extending above 850 hPa. The LI is used to determine the stability or instability of the lower part of the troposphere. It is obtained by computing the temperature difference between an air parcel lifted dry adiabatically from the ground to the lifting condensation level (LCL) and then pseudo-adiabatically to 500 hPa, and the temperature of the environment at 500 hPa. The risk of thunderstorms and severe weather activity are defined as the LI becomes negative (the more negative, the more unstable the air is, and the stronger the updrafts are likely to be with any developing thunderstorms). Similar to SI, the LI assesses the (in)stability at one level of middle troposphere and not the (in)stability of the entire troposphere, as does the CAPE.

The TT index measures the total effect of vertical temperature lapse rate and low level moisture and it is defined as the sum of two other indices: (1) the VT index and (2) the CT index (strongly influenced by the 850-hPa moisture). However, the TT does not assess any shear, it

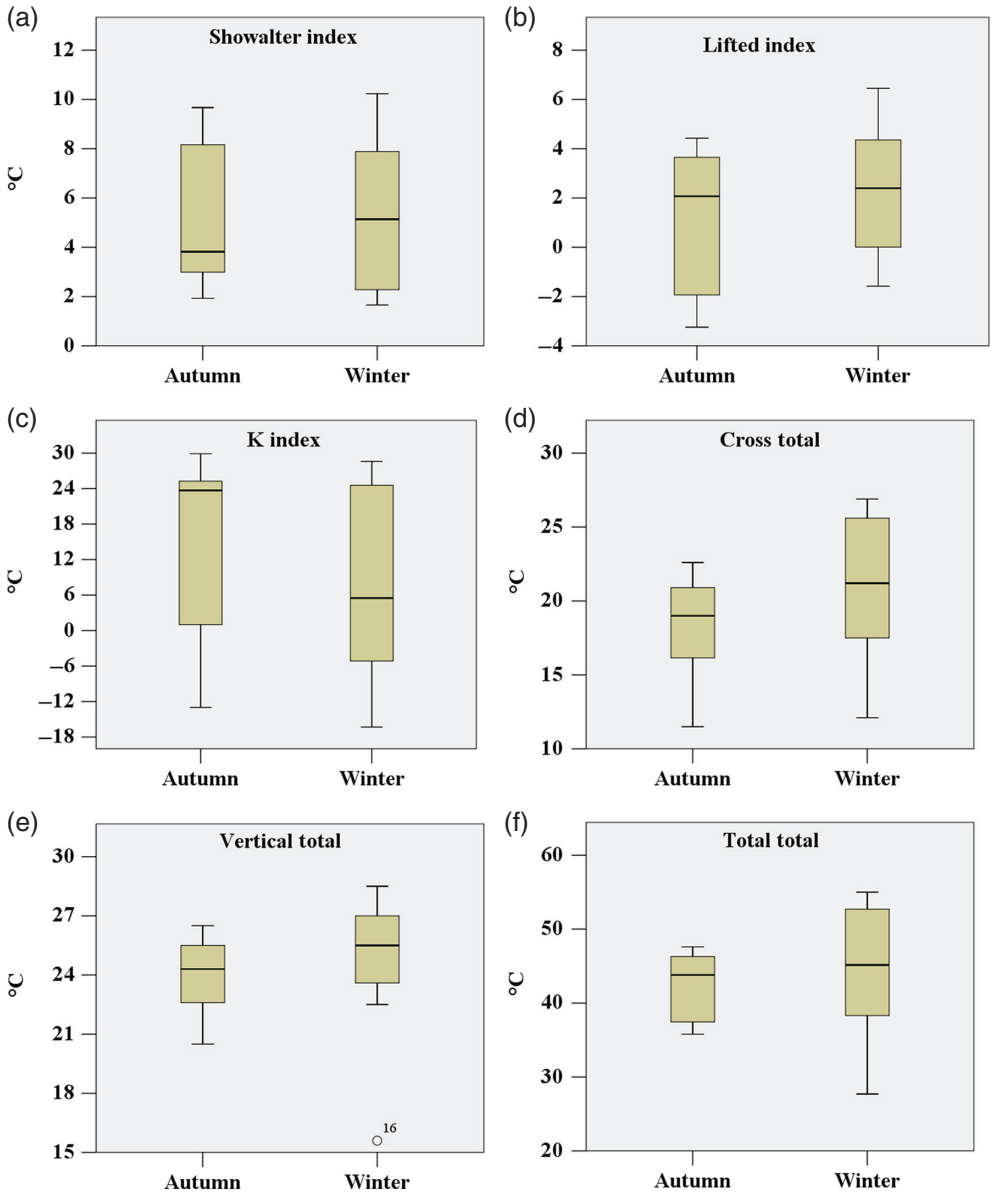

Figure 5. Similar to Figure 4, but for the following instability indices: (a) SI, (b) LI, (c) K-index, (d) CT index, (e) VT and (f) TT.

may not account for a capping inversion (that prevents storms from developing), and if there is a layer of moisture below 850 hPa the index will be too stable. The K-index is a combination of the VT and lower tropospheric moisture characteristics, as the K-index measures thunderstorm potential based on vertical temperature lapse rate, moisture content of the lower atmosphere and the vertical extent of the moist layer. SWEAT index discriminates between ordinary and severe convection by incorporating its thermodynamic and kinetic function mechanism. The BRN expresses the buoyant energy (instability) given by CAPE compared to the vertical wind shear (speed and directional shear with height) in a thunderstorm environment. CAPE is the amount of energy a parcel of air would have if lifted vertically above the level of free convection (LFC) through the atmosphere. Thus, CAPE is effectively a measure of the vertically integrated positive buoyancy of an air parcel and it is an indicator of atmospheric instability, which makes it valuable in predicting severe weather. On the other hand, CIN is the amount of energy required to overcome the negative buoyancy force the environment exerts on an air parcel.

It is evident that the value of above-described indices is strongly associated with their capacity to summarize in a single number some characteristics of the severe storm environment. However, operational forecasters have to consider the full complexity of four-dimensional atmospheric data (Doswell and Schultz, 2006). But, the press of time can encourage severe operational forecasters to use these indices to obtain a quick 'look' at the data for the purpose of identifying the hot spots upon which to focus more attention on nowcasting (Doswell and Schultz, 2006). CIN and CAPE are considered more useful diagnostic indices by operational forecasters and researchers as they are a measure of the buoyancy throughout the entire troposphere.

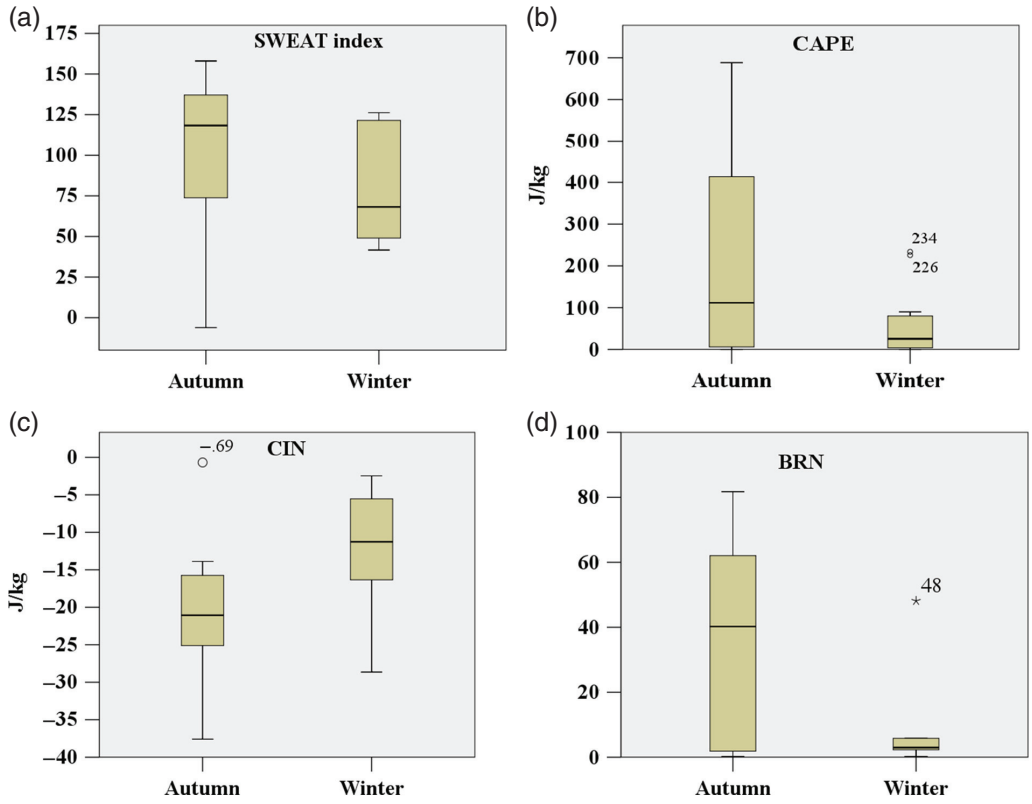

Figure 6. Similar to Figure 5, but for the following instability indices: (a) SWEAT, (b) CAPE, (c) CIN and (d) BRN.

Table 2. Seasonal minimum, maximum and median values of SST (in °C), LCL (hPa), LFC (hPa) and mean EL (hPa) for waterspout and non-waterspout days over the southern Aegean Sea during 2005–2012.

Season		Waterspout days				Non-waterspout days			
		LCL (hPa)	LFC (hPa)	EL (hPa)	SST (°C)	LCL (hPa)	LFC (hPa)	EL (hPa)	SST (°C)
Autumn	Minimum	833	728	225	16.5	671	388	202	17.6
	Maximum	939	933	609	25.4	962	953	886	26.4
	Median	893	833	338	24.2	893	835	501	21.8
Winter	Minimum	838	787	357	15.2	614	553	255	14.21
	Maximum	948	925	856	19.1	987	987	940	9.4
	Median	891	851	617	17	887	867	750	16.1

The seasonal distributions of thermodynamic instability indices (described in Section 2) during autumn and winter waterspout days are shown in Figures 5 and 6 by means of box-and-whisker plots. The SI (Figure 5(a)) during autumn waterspout days (left variable) varied from 1.9 to 9.4 °C; however, the distribution was skewed towards colder temperatures. During winter (right variable), the distribution was symmetrical about the median at 5.1 °C, with the upper (lower) whisker at 10.7 (1.7 °C). The LI (Figure 5(b)) during autumn ranged from −2.7 to 4.8 °C with a median of 2.2 °C; the distribution is skewed towards warmer temperatures. However, during winter the LI distribution was not skewed, varying from −1.5 to 6.8 °C with a median of 2.6 °C.

The K-index (Figure 5(c)) during autumn (winter) waterspout days ranged widely from −13.0 to 29.9 °C (−16.3 to 28.6 °C) with a median of 23 °C (8 °C). During autumn waterspout days, the CT and VT (Figure 5(d) and 5(e), left variable, respectively) varied from 11.5 to 22.6 and 20.5 to 26.5 °C, respectively. The TT (Figure 5(f), left variable) during autumn waterspout days varied from 35.8 to 47.6 °C. Compared to the autumn distribution, the CT and VT distribution during winter waterspout days was much broader, as the CT (VT) varied from 12.1 to 26.9 °C (22.6 to 28.5 °C), and as a result the TT (Figure 5(f), right variable) varies widely from 27.7 to 55 °C, during the winter.

The SWEAT index (Figure 6(a)) during autumn waterspout days (left variable) varies more widely (0–165) than in winter (40–130) (right variable). Similar to the SWEAT, the CAPE during autumn varied more than during winter. The autumn CAPE median was 108 J kg^{-1} with maximum values at 700 J kg^{-1}, as compared to just 30 J kg^{-1} with a maximum of 240 J kg^{-1} in winter (Figure 6(b)). However, the CIN during winter waterspouts days was lower (less negative) than in autumn. Thus, the kinetic energy needed to lift an air parcel from the surface to its LFC is higher

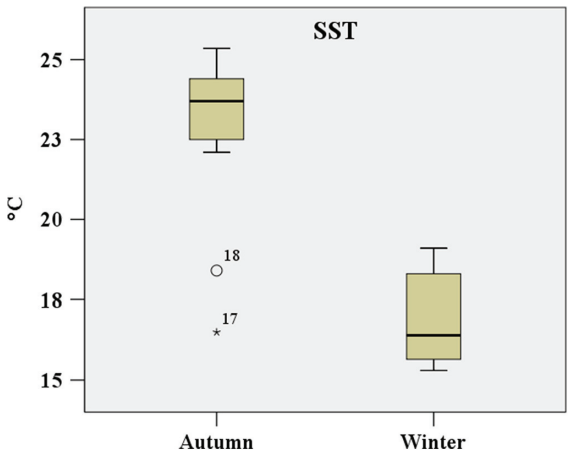

Figure 7. Similar to Figure 4, but for the SST. SST data were derived from the NCEP/MMAB.

during the autumn (Figure 6(c)). This suggests that autumn cases are more favourable to the development of convection in terms of CAPE, while in winter the inhibition is less and the smaller instability can be released more easily. The BRN index during autumn has a median of 40 and a maximum of 85. However, during winter waterspouts days, the distribution is narrower and the maximum did not exceed 5 (Figure 6(d)).

Table 2 summarizes the seasonal distribution of LCL, LFC and equilibrium level (EL) during autumn and winter over the southern Aegean Sea. Results confirm that deeper convection is possible in autumn (higher EL) but it is relatively easier to be triggered in winter (lower median of LCL and LFC). The SST of the southern Aegean Sea (Figure 7) during autumn waterspout days varied from 16.5 to 25.4 °C; however, the SST for 95% of waterspouts events ranged from 22.0 to 25.4 °C. Compared to the autumn SST during winter waterspout days, the SST was much cooler (Table 2).

3.2. Seasonal analysis of wind, thermodynamic and SST data during non-waterspout days, 2005–2012

This section summarizes autumn and winter climatology of wind, thermodynamic and SST data during non-waterspout days, 2005–2012. In Figure 8, wind rose graphs are used to illustrate the frequency (%) distribution of wind speed ($m\,s^{-1}$) and wind direction (one tenths of a degree), during autumn non-waterspout days over the southern Aegean Sea, at the following pressure levels of 500 hPa (Figure 8(a)), 700 hPa (Figure 8(b)), 850 hPa (Figure 8(c)) and 925 hPa (Figure 8(d)). During winter non-waterspout days (not shown), at 500 hPa (700 hPa), the prevailing wind direction was from the W–SW (W–SW), while the wind speed varied from 10 to 40 $m\,s^{-1}$ (3–12 $m\,s^{-1}$). At 850 hPa (925 hPa), winds were mainly from the NW to SW (NW) at speeds up to 8–11 $m\,s^{-1}$ (mostly >7 $m\,s^{-1}$).

Regarding the air temperature distribution at middle and lower troposphere, at 500 hPa (not shown), during autumn (winter) non-waterspout days, the air temperature varied from −26.7 to −4.5 °C (−32.7 to −10.9 °C), with a median of −14.5 °C (−20.3 °C). The air temperature at 700 hPa (not shown) during autumn (winter) non-waterspout days varied from −10.1 to 11.6 °C (−13.7 to 7.6 °C), with a median of 3 °C (3.8 °C). At 850 and 925 hPa (not shown), during autumn (winter) non-waterspout days, the air temperature ranged from −3.7 to 24.4 and −2.6 to 30 °C (−7.3 to 20 and −1.1 to 24.6 °C), with a median of 11.2 and 14.8 °C (4.4 and 9.3 °C), respectively.

Figure 9 illustrates the seasonal distributions of thermodynamic instability indices during autumn and winter non-waterspout days, by means of box-and-whisker plots. The distribution of SI (Figure 9(a)) during autumn and winter non-waterspout days (left and right variable, respectively) was symmetrical about a median of 6.3 and 6.9 °C, with the upper (lower) whisker at 16.7 and 17.9 °C (−3 and −3.8 °C), respectively. The LI (Figure 9(b)) during autumn (left variable) ranged from −6.7 to 11.9 °C with a median of 2.7 °C. During winter (right variable), LI varied from −2.2 to 15.8 °C with a median of 4.8 °C.

The K-index (Figure 9(c)) during autumn (winter) non-waterspout days ranged widely from −41.5 to 37 °C (−42 to 39 °C) with a median of 10.6 °C (6.9 °C). The CT and VT (not shown) distribution was symmetrical during autumn (winter) non-waterspout days and varied from −10.9 to 27 °C (−20.5 to 27.5 °C) and 13.2 to 35.9 °C, respectively. The TT (not shown) during autumn and winter non-waterspout days ranged from 12.8 to 57.5 °C and 6 to 59.1 °C, with a median of 40.8 and 43 °C, respectively.

The SWEAT index (Figure 9(d)) during autumn non-waterspout days (left variable) varies more widely (10.9–270) than in winter (from 15 to 182) (right variable). Like the SWEAT, the CAPE during autumn varied more than in winter. The CAPE (Figure 9(e)) distribution during autumn (left variable) non-waterspout days was skewed towards lower values with a median of 66.5 $J\,kg^{-1}$ and upper whisker of 688 J/kg, against to just 17.3 $J\,kg^{-1}$ with an upper whisker of 110 $J\,kg^{-1}$ in winter (right variable). The CIN (not shown) during autumn non-waterspout days was higher (more negative) than in winter season. In particular, CIN during autumn (winter) varied from −270 to 0.1 $J\,kg^{-1}$ (−60 to 0.1 $J\,kg^{-1}$), with a median of −31.8 $J\,kg^{-1}$ (−11.1 $J\,kg^{-1}$). The BRN index (Figure 9(f)) during autumn (winter) has a median of 2.7 (1.1) and a maximum of 197 (250). The seasonal distribution of LCL, LFC, EL and SST for non-waterspout days are presented in Table 2.

3.3. Temporal analysis of the MSG CTT data during waterspout days

The analysis of CTT in terms of BT (K) is presented for waterspout days for both radii (R_1 and R_2), although the summer analysis was excluded because the sample size for waterspout days included only 1 day. The CTT analysis is presented for the evolution of the minimum BT over a 2-h period, from 60 min prior to 60 min after waterspout formation. Hereafter, T_0 refers to the time of waterspout formation, T_{-XX} to the XX time (min) prior to waterspout

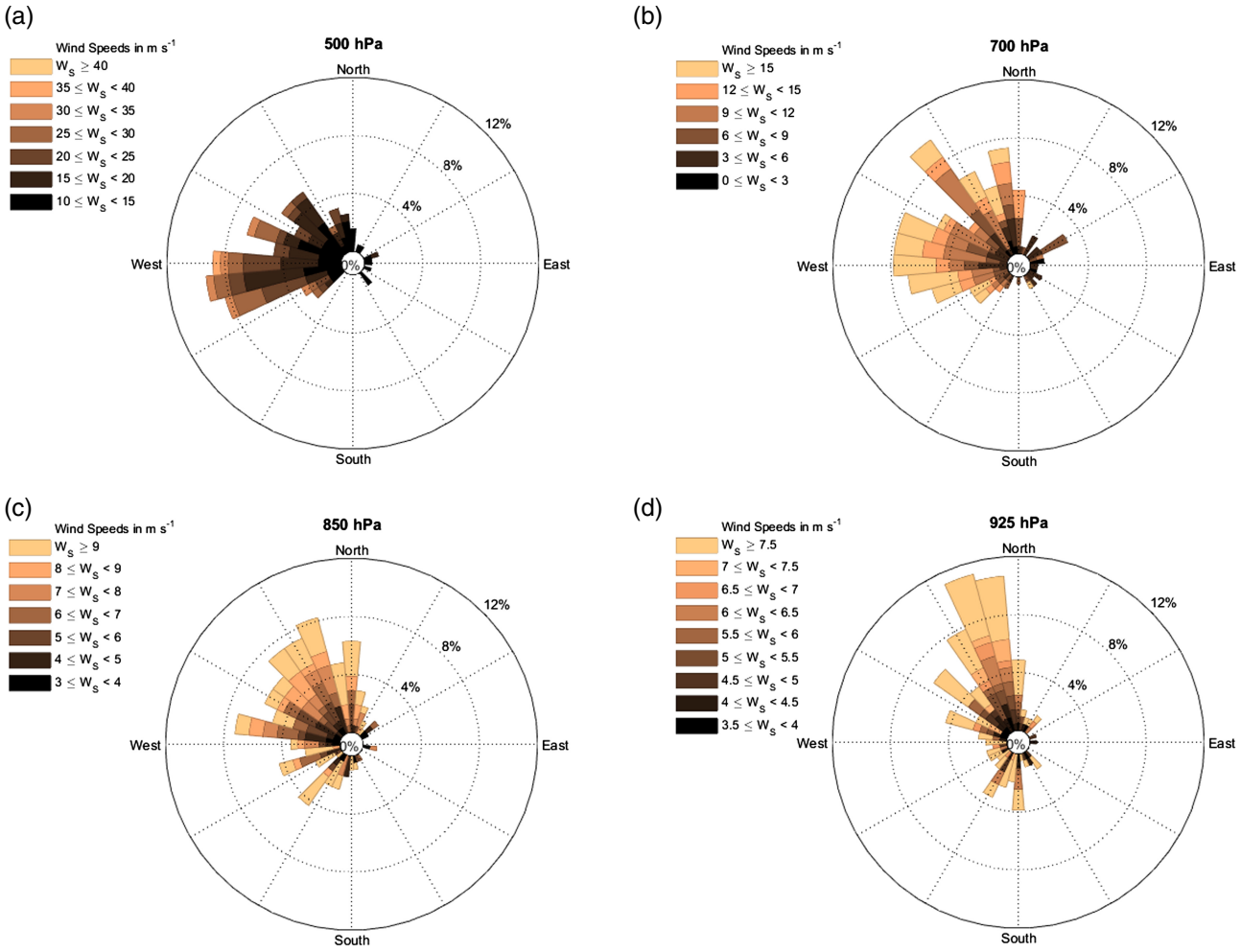

Figure 8. Similar to Figure 3, but for the non-waterspout days during autumn 2005–2012.

formation, and T_{+XX} to the XX time (min) after waterspout formation. In Figures 10 and 11, seasonal box-and-whisker plots are used to compare the minimum BT distribution within the 2-h analysis window for R_1 and R_2, respectively.

During autumn waterspouts days, for R_1, there was a gradual decrease of median BT (from 272–250 K) starting during the T_{-60} to T_{+30} time window (Figure 10(a)). The highest BT is estimated to be 290 K and the minimum BT is 215 K. The value of the 75th percentile of BT, close to waterspout formation time, was about 275 K. The autumn BT distribution during the T_{-60} to T_{-15} time window was approximately symmetric about the median. During winter waterspout days, the median BT did not change significantly prior to and after the waterspout event (Figure 10(b)). In particular, the median varied only from 255 to 245 K. Furthermore, the T_{-15}, T_0 and T_{+15} box plots were narrower (255–240 K) than the other BT box plots (265–235 K). The median of BT during spring waterspout days was higher than in winter and autumn. The BT distribution during spring waterspout days was narrower close to waterspout formation time than during the other seasons (Figure 10(c)).

During autumn waterspout days, the median of BT for R_2 decreased significantly between T_{-45} and T_{-30} (265–240 K) (Figure 11(a)). The BT distribution is skewed towards colder values after T_0. The BT median during winter waterspouts days (Figure 11(b)) did not change much with time. However, during the T_{-15} to T_0 time window, there was a slight decrease in the BT and the BT distribution was skewed towards warmer temperatures after waterspout time T_0. During the spring (Figure 11(c)), there was a warmer and narrower distribution of BT and the median was 270 K.

As in the BT analysis, the seasonal frequency (%) of observed CBH (m) waterspout parent cloud, during a 30-min time window of the waterspout event (at T_0 time), derived from HNMS Heraklion weather observations (METAR) during waterspout days over the coasts of Heraklion, is presented in Table 3. During autumn waterspout days, the dominant (92.3%) CBH was observed between 500 and 700 m; however, lower CBHs (<500 m) were observed for a few (7.7%) waterspout case studies. On winter waterspout days, the lowest CBH was <300 m, but the commonly observed CBH was again in the 500–700 m range. As in autumn and winter, the CBH during spring was most common between 500 and 700 m; however, CBH was also higher (lower) than 700 m (500 m). Thus, although in spring the majority of the events

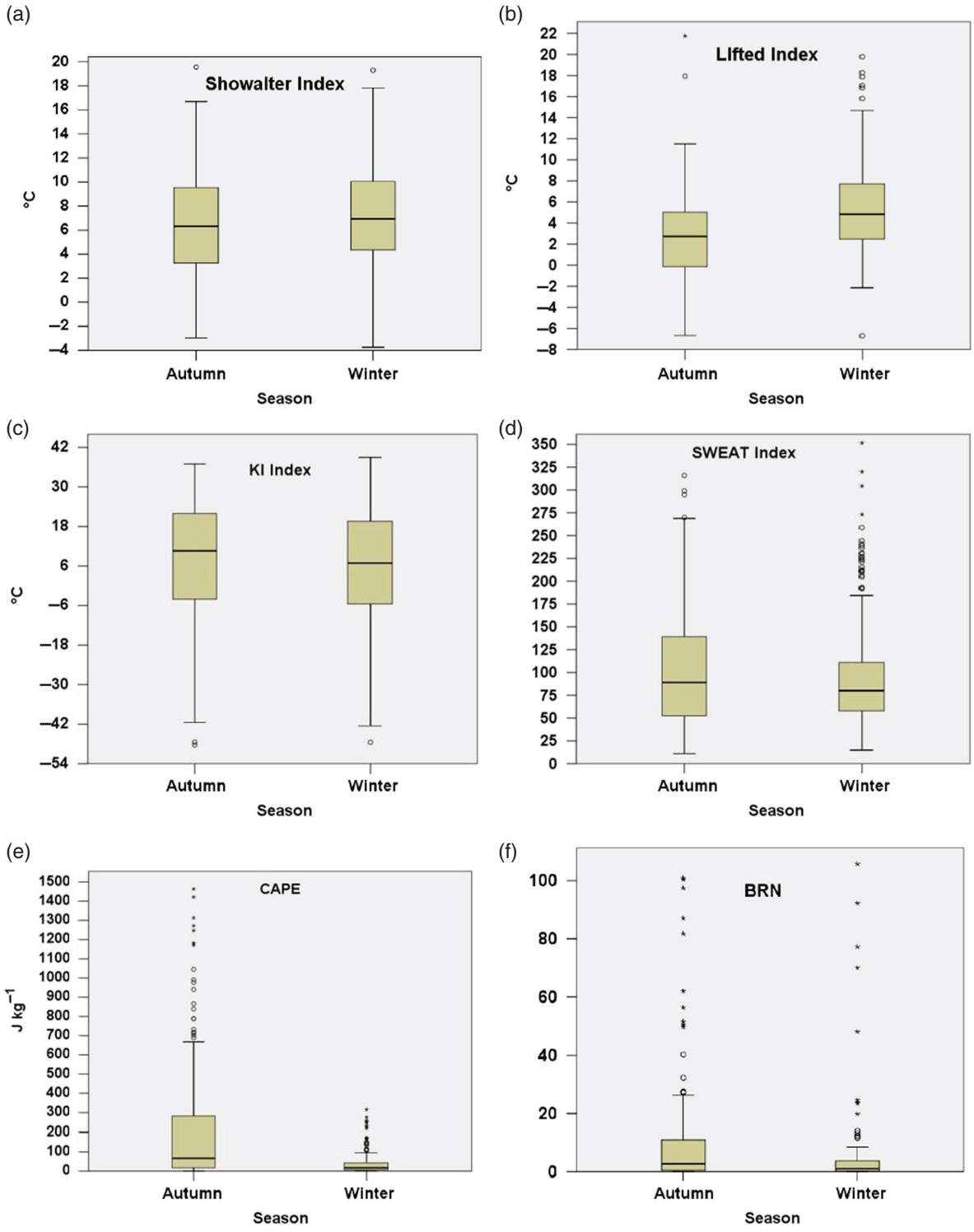

Figure 9. Similar to Figure 4 but for the following instability indices: (a) SI, (b) LI, (c) K-index, (d) SWEAT, (e) CAPE and (f) BRN during autumn (left variable) and winter (right variable) non-waterspout days, for over the southern Aegean Sea, 2005–2012.

occurred in the same category, the presence of some cases at higher levels suggest the different characteristics of the events in this season.

4. Discussion

In Figure 12, box-and-whisker plots are used to depict the wind direction distribution during autumn (left variable) and winter (right variable) waterspout days, over the southern Aegean Sea. Our findings of prevailing northwesterly winds at 500 hPa are in agreement with Matsangouras *et al.* (2014), who showed that a very broad trough at 500 hPa was located over the Aegean Sea, resulting in W–NW upper air flow over Crete on autumn waterspout days during the period covering 1 September 1948–31 December 2012. However, the occurrence of

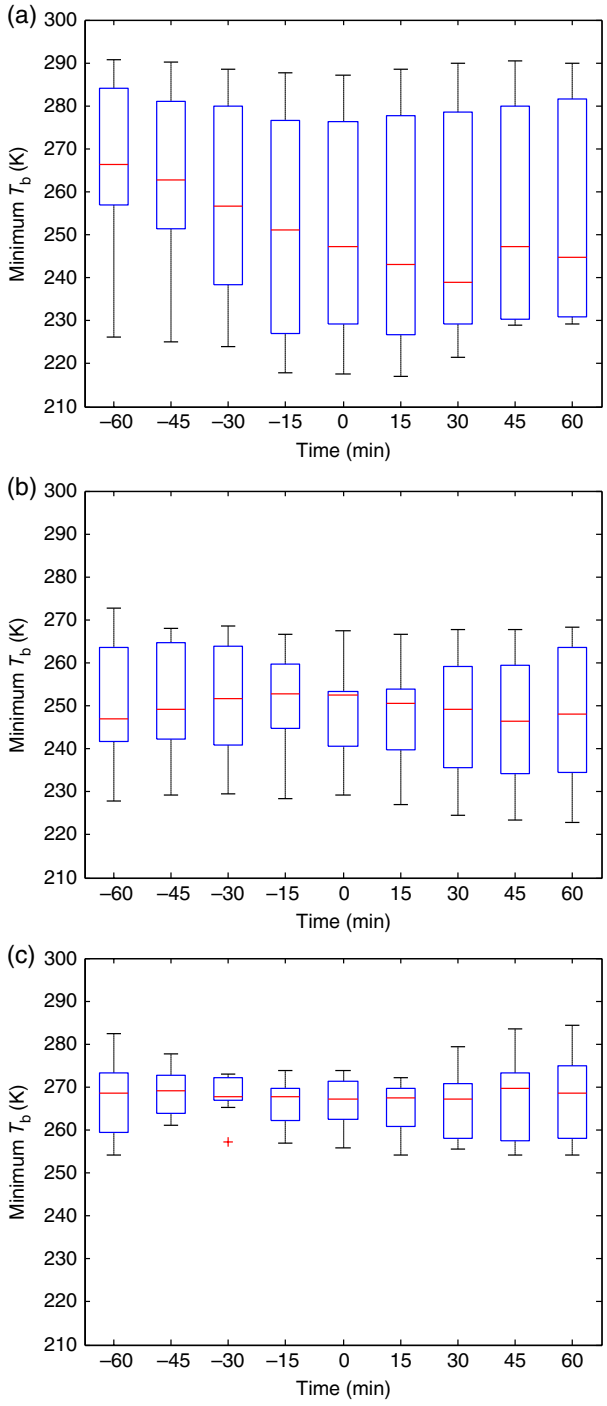

Figure 10. Box-and-whisker plots of minimum BT distribution (K) at 60 min prior and 60 min after waterspout formation, for R_1 search radius, during autumn (a), winter (b) and spring (c) waterspout days over the southern Aegean Sea (2005–2012). In each plot, boxes show the upper (75th percentile) and lower (25th percentile) percentile, the horizontal line is the median and whiskers are the range of results.

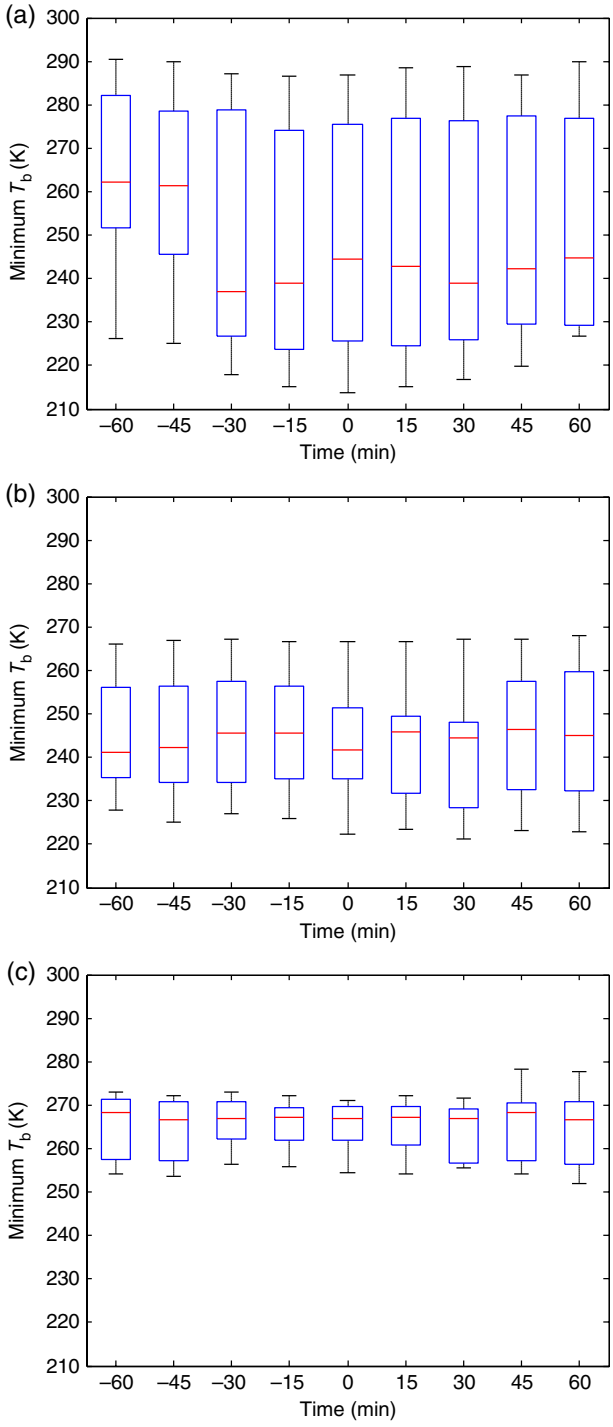

Figure 11. Similar to Figure 10, but for R_2 search radius.

northwesterly winds that favoured waterspout activity during the autumn season, at middle and lower levels of the troposphere over the southern Aegean Sea, differs from the SW upper and lower air flow that favours waterspout activity over western Greece (Nastos and Matsangouras, 2014a). Northwesterly winds in autumn at 850 and 925 hPa are consistent with a shallow, cyclonic circulation over the SE Aegean Sea. Like the synoptic conditions at 850 and 925 hPa, there is a shallow cyclonic circulation over the SE Aegean Sea, that extends down to sea level, consistent with N–NW surface streams over the north coast of Heraklion City.

In addition, our wind direction composites for winter are similar to those of Matsangouras and Nastos (2013) and Nastos and Matsangouras (2014b), who investigated seasonal composite synoptic conditions during waterspout days over the southern Aegean Sea. In winter, the westerly–southwesterly air flow at 500 and 850 hPa

Table 3. Seasonal frequency (%) of observed waterspout parent CBH (m) during a 30-min time window of waterspout event (at T_0 time), derived from HNMS Heraklion weather observations (METAR) during waterspout days over the coasts of Heraklion.

CBH (m)	Frequency (%)								
	Autumn			Winter			Spring		
	T_{-30}	T_0	T_{+30}	T_{-30}	T_0	T_{+30}	T_{-30}	T_0	T_{+30}
CBH ≤ 300	–	–	–	9.1	9.1	9.1	–	–	–
300 < CBH ≤ 500	7.7	7.7	7.7	–	–	–	22.2	11.1	11.1
500 < CBH ≤ 700	92.3	92.3	92.3	90.9	90.9	90.9	66.7	77.8	77.8
CBH > 700	–	–	–	–	–	–	11.1	11.1	11.1

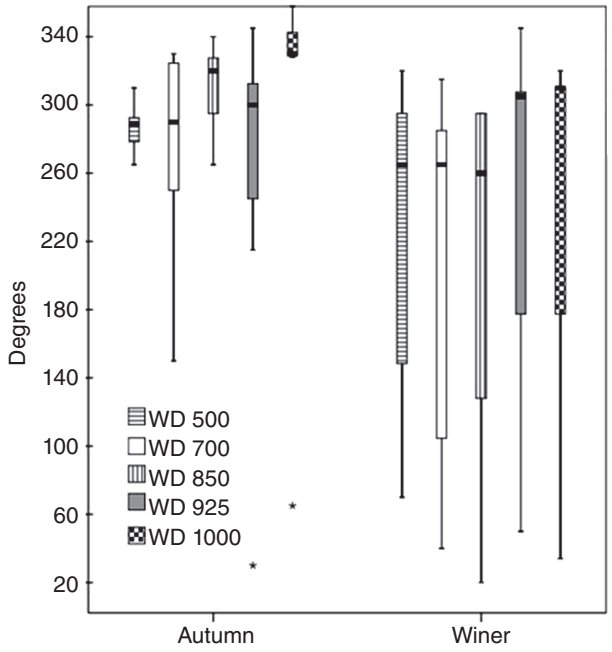

Figure 12. Box-and-whisker plots of wind direction, during autumn (left variable) and winter (right variable) waterspout days, at 500 hPa (white with grey horizontal lines), 700 hPa (white), 850 hPa (white with grey vertical lines), 925 hPa (grey) and 1000 hPa (white with black boxes) over the southern Aegean Sea. On each box, the central mark (black line) is the median, the edges of the box are the 25th and the 75th percentiles, while the whiskers extended to the most extreme data points and outliers are plotted individually (asterisks or circles). Upper air data, during waterspout days, were based on upper air soundings from HNMS Heraklion meteorological station (WMO ID: 16754).

originates from a trough axis located along the SW Ionian Sea. However, from the significantly broader wind distribution at all levels during winter (2005–2012), it is found that waterspouts also developed under the influence of S–SE air flow. Indeed, research based on an objective synoptic classification of waterspout days over Greece by Matsangouras *et al.* (2013) is in agreement with the finding that waterspouts are also reported under the influence of SW air flow at 500 hPa (a long-wave trough extends from Corsica to the north coast of Africa) and S–SE air flow at sea level (a closed cyclonic circulation over Sicily). A seasonal statistical analysis, based on the statistically significant differences ($p < 0.01$) between the values of wind direction (W_D) and wind speed (W_S) of the lower and middle levels of the troposphere for waterspout *versus* non-waterspout days during 2005–2012, was conducted. The results revealed that there is a statistically significant difference between the means of the following parameters for the waterspout and non-waterspouts days over the southern Aegean Sea during autumn: (1) W_D and W_S at 1000 hPa, (2) W_S at 925 hPa, (3) W_D and W_S at 850 hPa, (4) W_D at 700 hPa and (5) W_D 500 hPa. On the contrary, there is no statistically significant difference between means of the parameters W_D and W_S during winter season.

Sioutas (2011), using tornado and waterspout events in Greece from 2000 to 2009, found the following four basic synoptic patterns associated with tornado and waterspout occurrence over Greece: (1) southwest flow, (2) long-wave trough, (3) short-wave trough and (4) closed low. Sioutas (2011) found that the short-wave trough pattern is the most common synoptic pattern on waterspout days, followed by the closed low pattern. However, research by Nastos and Matsangouras (2012, 2014a) and Matsangouras *et al.* (2014) over different geographical areas of Greece showed that waterspouts and tornadoes in Greece are reported for a variety of different synoptic conditions. Thus, an objective synoptic classification based on regional clustering of the waterspout and tornado events is necessary in order to interpret synoptic conditions that favour waterspout and tornado development over a specific geographical area. Our results are similar to the preliminary results of Matsangouras *et al.* (2013), who showed that they could be used by operational forecasters in HNMS.

The LI seasonal distributions are skewed towards higher values, which suggest stable conditions. However, more waterspout days with an LI of <0 °C were found during autumn than in winter, suggesting marginally unstable or slightly unstable conditions. Sioutas (2011), based on 2000–2009 waterspout events in Greece, found that the LI (K-index) varied from −13 to 5 °C (−11 to 34 °C) and the mean was −1.6 °C (21.7 °C). Although our results fall within Sioutas' range, we have found that waterspouts over the southern Aegean Sea are possible under more stable or marginally unstable condition than in other region of Greece. Regarding the K-index, more than 50% of waterspout events during autumn took place with a K-index in excess of 23 °C.

As the TT measures the total effect of vertical temperature lapse rate and low level moisture, we found that more than 50% of waterspout over the southern

Aegean Sea developed when the TT index was higher than 45 and 46 in the autumn and winter, respectively. Based on this analysis, it may be inferred that more than 50% of waterspouts events occur under scattered shallow convective-cloud conditions. This inference is in agreement with the IR image analysis for waterspout days, since cumulus lines were detected on IR images close in time to waterspout formation. SWEAT index of seasonal distribution is indicative of a shallow convection rather than a typical tornado environment, as the SWEAT incorporates both thermodynamic and kinematic attributes of the middle and lower troposphere. Based on the SWEAT and the CAPE, during autumn waterspout days, it may be also inferred that there is a similar shallow-convection environment. On the other hand, there is significantly lower CAPE ($<100\,\mathrm{J\,kg^{-1}}$) in the winter, suggesting unfavorable conditions for convective weather. Since the BRN is a parameter that assesses the relative amount of thermodynamic instability (in terms of CAPE) to wind shear in an unstable environment, we expected the BRN to be significantly lower (<10) during winter waterspout days, while indicating unstable weather conditions for autumn.

Research by Sioutas (2011), based on waterspout events in Greece from 2000 to 2009, in which the thermodynamic characteristics of waterspout days were calculated, found that the mean (minimum/maximum) values of CAPE, SWEAT and BRN were $762\,\mathrm{J\,kg^{-1}}$ (0/$2875\,\mathrm{J\,kg^{-1}}$), 138.9 (31/326) and 149.7 (0/682), respectively. Our findings indicated that more than 50% of waterspout activity over the southern Aegean Sea was favoured under more thermodynamically stable weather conditions than the other parts of Greece. The LCL seasonal distribution (not shown) is characterized as symmetrical about the median at 915 hPa. However, since the EL was significantly higher during autumn than winter, there is greater thermodynamic instability and higher CAPE during autumn.

Regarding the statistically significant differences ($p < 0.01$) between the values of the above-mentioned thermodynamic instability indices during waterspout days *versus* non-waterspout days during 2005–2012, the analysis showed that the differences between the means of the following parameters are statistically significant ($p < 0.01$) for the development (or not) of waterspout over the southern Aegean Sea during autumn: SI, LI, K-index, SWEAT, BRN, CT, TT index and CIN. However, during winter, the differences between the means of the above-mentioned instability indices for waterspout days and non-waterspout days are not statistically significant.

Warmer conditions were found on autumn waterspout days than on winter waterspout days. A new instability parameter, the ΔT^{1000} (the temperature difference between that at 1000 hPa and that at 500, 700, 850 and 925 hPa) exhibited a symmetrical distribution about the median for both seasons, at all pressure levels. In Figure 13, the autumn and winter ΔT^{1000} distributions on waterspouts days over the southern Aegean Sea are shown for selected pressure levels. From box-and-whisker plots, it is seen that

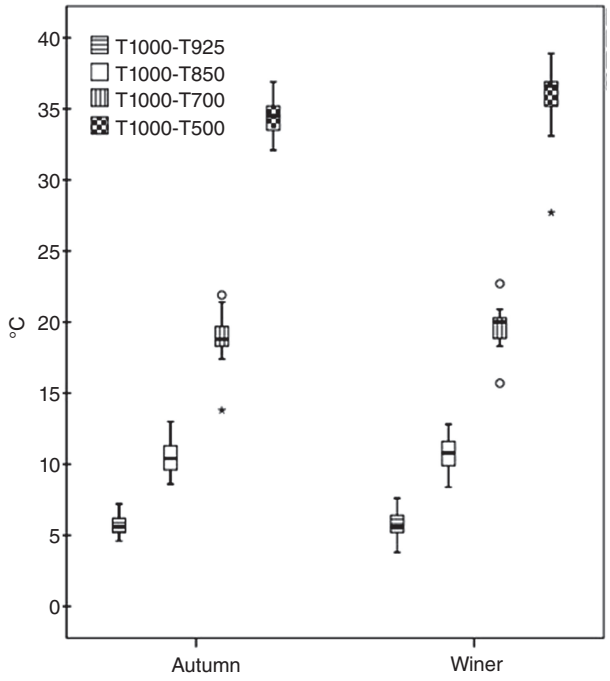

Figure 13. Similar to Figure 12, but for the ΔT distribution at specific pressure level. ΔT is the instability index defined as the temperature difference between 1000 hPa and specific pressure level.

the range in ΔT^{1000} is <2 and $<3\,^{\circ}\mathrm{C}$ at lower and middle levels of the troposphere, respectively; it follows that more than 50% of waterspout activity over the southern Aegean Sea occurred for different weather conditions during each season. Moreover, this almost constant (with small variance) temperature difference during autumn and winter could be used as a component of a forecasting tool for the autumn and winter waterspout activity over the southern Aegean Sea. Kamperakis *et al.* (2014), using a data mining method applied on European Centre for Medium-Range Weather Forecasts reanalyis data set, showed that the relative humidity at the pressure levels of 700 and 925 hPa, and the difference of temperature between 700–925 and 700–850 hPa revealed to be the most crucial attribute contributors for waterspout development over the southern Aegean Sea.

Aside from the synoptic conditions that favour tornadic events, factors, such as the varying depth of the sea, sea currents, different shapes of the coastline and SST (Carapiperis, 1952), are all likely to contribute to the conditions favourable for the development of tornadoes and waterspouts. The southeast Aegean is affected by the influx of Levantine waters, mainly through the Rhodes passage. This Levantine water mass travels northwards along the eastern Aegean Sea, close to the coasts of Asia Minor, having no impact in the central Aegean Sea. Additionally, the role of surface currents is significant in configuring the spatial distribution of SSTs. Aegean's SST fluctuates spatially and seasonally; mean monthly SSTs range from as low as $8\,^{\circ}\mathrm{C}$ in the north during winter to as high as $26\,^{\circ}\mathrm{C}$ in the south during late summer (Poulos *et al.*, 1997). The overall seasonal spatial distribution

of the SSTs over the Aegean Sea depends on the following: (1) the distribution of the colder waters from the Black Sea; (2) the advection of the warmer Levantine Waters, which influences only the eastern part of the south and central Aegean; (3) coastal upwelling induced by the Etesian winds, which are periodic northerly winds in the lower troposphere that flow over the Aegean Sea during summer and early autumn and are the consequence of a low-pressure system that extends from Turkey to northwest India and of a high-pressure centre in the central and south Europe (Metaxas and Bartzokas, 1994) and (4) to a lesser extent but locally important (especially in the north), freshwater riverine outflows (Poulos *et al.*, 1997). Our findings regarding the SST autumn (winter) distribution are that more than 75% of autumn (winter) waterspout activity over the southern Aegean Sea developed with SSTs varying from 22.0 to 24.5 °C (15.3–18.0 °C). Research by Golden (2003), based on 10 years of (1958–1968) waterspout data from Key West, Florida, USA, indicated a significant increase of waterspout activity when SSTs were in excess of 25 °C. Thus, SST seems to be a factor contributing to geographic variations in waterspout activity.

Similar to the index ΔT^{1000}, but using the SST instead of air temperature at 1000 hPa, a new thermodynamic parameter was introduced to our data set, the ΔT^{SST}. In Figure 14, the ΔT^{SST} autumn (left variable) and winter (right variable) distributions are similar to the ΔT^{1000} distributions. In particular, ΔT^{SST} varies less in the lower troposphere than in the mid-troposphere. Szilagyi (2009), investigating 14 parameters as possible predictors for waterspout formation over the Great Lakes in the USA, found that among these (1) the water − 850 hPa temperature difference and the (2) convective cloud depth (EL–LCL) were positively correlated with the potential for waterspout development; and that (3) wind speeds at 850 hPa must be $<20\ m\ s^{-1}$. Keul *et al.* (2009), testing the Szilagyi's nomogram for waterspout activity over the Aegean Sea (2002–2006), showed that 75% of waterspouts satisfied Szilagyi's (2009)criteria for the Great Lakes. However, the first parameter of Szilagyi's nomogram for waterspout activity over the southern Aegean Sea could not be verified (compared with other parts of Greece), as more than 75% of waterspouts are associated with $\Delta T^{SST} < 15$ °C (difference with temperature at 850 hPa) and convective-cloud depth (EL–LCL) is lower than 7000 m. Sioutas *et al.* (2013) showed that waterspout outbreaks are strongly related to the Szilagyi's waterspout index, which varies from 3 to 7, for the Aegean and Ionian Seas. The values of the Szilagyi waterspout index (SWI) ranged from −10 to +10, with waterspouts most likely to occur when SWI ≥ 0. Moreover, our statistical analysis showed that the differences between the means of the following parameters are statistically significant ($p < 0.01$) for the occurrence (or not) of waterspout over the southern Aegean Sea during the autumn: (1) SST, (2) SST–T700 hPa and (3) T1000–T700 hPa. However, during winter, the differences between the means of the above-mentioned parameters for waterspout days and non-waterspout days are not statistically significant, during 2005–2012.

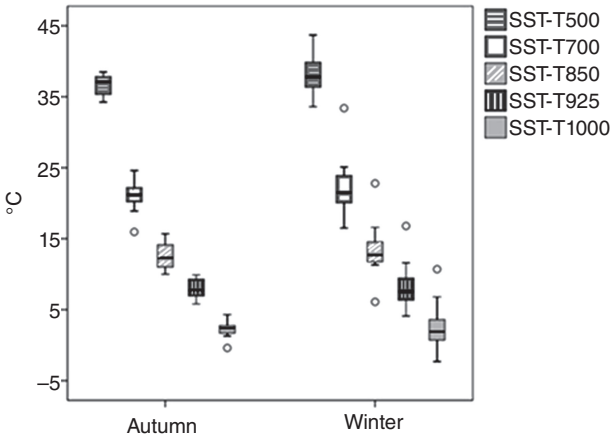

Figure 14. Similar to Figure 12, but for the SST.

It is known that although waterspouts develop in supercells and intense multicell squall lines, they can also develop under rather benign synoptic conditions (Hurd, 1950; Brooks, 1951; Price and Sasaki, 1963). As a result, waterspouts frequently originate from cumulus clouds with tops of only 3–6 km above mean sea level (Peterson, 1963; Woodley *et al.*, 1967; Golden, 1968, 1971, 1974b). Golden (1974b, 2003) estimated from his 1968–1972 Key West waterspout data set that 90% of waterspouts were spawned by rapidly building cumulus cloud lines, not isolated cumuli, suggesting that the cloud-line scale (mesoscale) is perhaps most crucial to waterspout formation. In fact, in our study, it was found from the satellite image analyses in the visible and IR spectrum channels, close to waterspout formation time, that waterspouts in Greece are also spawned by cumulus cloud lines. Golden (1974b) using a scaling procedure (Golden, 1974a) detailed estimates of the vertical growth rate of cloud turrets and bubbles; he divided the cloud line into three sections in order to relate cloud growth to waterspout formation. The average vertical growth rate throughout the cloud line exhibited a systematic increase in convective updraft strength during waterspout formation. Moreover, Golden (1974b) investigating the differences in cloud-line structure between waterspout-active and non-waterspout cumulus cloud lines showed that the maximum cloud tops in the waterspout-active cloud line grew from 3700 m to at least 5200 m during a 12-min span. Our findings, regarding CTT, are in agreement with those of Golden (1974b) in that a gradual decrease of CTT was detected over the southern Aegean Sea on waterspout days, suggesting an increase in the height of the cloud lines close to waterspout formation time. In autumn in particular, significant vertical development was found, indicating a vertical growth of the waterspout parent cloud. The decrease of CTT is most pronounced during autumn for both search radiuses.

5. Summary and conclusions

In this study, a recent LACAE's database of waterspout activity over the southern Aegean Sea is examined and a

summary of the climatology of the thermodynamic environment, synoptic conditions and SST during waterspout days is presented. In addition, a seasonal analysis of CTT using spaceborne data from the MSG satellite image data product is presented, in which the CTT time evolution of waterspout parent clouds, close in time to waterspout formation, is detailed. For the CTT analysis, 110 waterspout events on 26 waterspout days were considered during the time period from 8 March 2005 to 14 November 2013. The evolution of BT (every 15 min) during a 2-h period (±60 min regarding each waterspout event) was documented.

In our study, a daily, high-resolution, real-time, global SST analysis (developed by the NCEP/MMAB) with a spatial operational grid analysis of 1/12° was used over the southern Aegean Sea. We took into consideration waterspout events from 27 September 2005 to 31 December 2012. Rawinsonde data were used from the Heraklion upper-air meteorological station in order to examine the vertical profile of temperature, moisture and wind in the middle and lower troposphere on waterspout days over the southern Aegean Sea. Atmospheric variables (e.g. wind direction and speed, and temperature) were estimated at 500, 700, 850, 925 and 1000 hPa. The following indices were employed to quantify the unstable conditions during waterspout activity: CAPE, BRN, LI, SI, K, VT, CT, TT and CIN.

Based on the CTT and CBH analyses for waterspout development over the southern Aegean Sea, our main findings are as follows:

- The CTT of waterspout parent clouds decreased near the waterspout formation time, suggesting a vertical growth of clouds.
- The decrease of CTT with time was the greatest during the autumn.
- All waterspouts formed under lines of cumulus clouds.
- Our findings regarding the vertical growth of the parent cloud and the cloud-line structural features are in agreement with those of Golden (1974b).
- The CBH generally varied from 500 to 700 m; however, CBH was lower (<300 m) and higher (>700 m) during the winter and spring, respectively.

Our main findings based on the thermodynamic and synoptic conditions are as follows:

- Northwesterly winds predominate in autumn, which is in agreement with the composite synoptic analyses of Matsangouras *et al.* (2014). However, this pattern of northwesterly winds at middle and lower levels of the troposphere over the southern Aegean Sea differs from the southwesterly upper and lower air flow found over western Greece (Nastos and Matsangouras, 2014a), suggesting that different synoptic conditions are associated with waterspout activity over the water bodies of Greece. Winter waterspouts over the northern coasts of Heraklion City also developed under the influence of S–SE air flow, in line with the results of Matsangouras and Nastos (2013) and Nastos and Matsangouras (2014b). The SI on autumn and winter days was not suggestive of high thermodynamic instability over the southern Aegean Sea, which is in agreement with Sioutas (2011).
- More than 50% of waterspout events in autumn took place while the K-index was >23 °C, indicating shallow convection.
- More than 50% of waterspouts over the southern Aegean Sea developed when the TT index was greater than 45, during autumn.
- The SWEAT, BRN and CAPE during autumn were suggestive of a shallow-convection environment with a higher EL, in contrast to winter, when there were less favourable convective conditions and a significantly lower EL.
- Not surprisingly, the troposphere is warmer in autumn than in winter. However, the instability parameter ΔT^{1000} had a symmetrical distribution about the median for both seasons and at all pressure levels.

Finally, from the SST analyses, the following results were found:

- More than 75% of autumn (winter) waterspout activity over the southern Aegean Sea developed with SST values varying from 22 to 24.5 °C (15.3–18 °C).
- The instability parameter ΔT^{SST} had a symmetrical distribution about the median for both seasons and at all pressure levels, consistent with the ΔT^{1000} seasonal distribution.
- The differences between the means of the parameters W_D and W_S at 1000 and 850 hPa, W_S at 925 hPa, W_D at 700 and 500 hPa, SI, LI, K-index, SWEAT, BRN, CT, TT, CIN, SST, SST–T700 hPa and T1000–T700 hPa between waterspout and non-waterspout days are statistically significant ($p < 0.01$) during autumn.

Future research regarding waterspout activity over the southern Aegean Sea is planned in order to develop a numerical approach to introduce a forecast tool that will adopt an objective synoptic classification based on regional (geographical) clustering of waterspout and tornado reports and our seasonal threshold findings of instability indices, thermodynamic parameters as well as wind components.

Acknowledgements

All authors contributed extensively to the work presented in this paper. I.T.M, jointly conceived the concept with P.T.N and H.B.B. and prepared the manuscript. K.P and I.T.M. analysed the MSG data. I.P., M.M.M., P.T.N, I.T.M. and H.B.B. performed the analysis of remote sensing data. The authors acknowledge EUMETSAT, the University of Wyoming, the NCEP/MMAB and the HNMS for the data used in our analyses. Also, this study was partially completed under the postgraduate programme 'Environmental Physics' co-funded by the Action 'State Scholarships

Foundation (SSF/IKY) programme with an individualized evaluation process for the academic year 2011–2012' with ID 2011-1-280 from the resources of the operational programme 'Education and Lifelong Learning' of the European Social Fund (ESF) and of the 'National Strategic Reference Framework (NSRF), 2007–2013'. A small part of this work was supported by National Science Foundation (NSF) grant AGS-1262048.

References

Bluestein HB. 2013. *Severe Convective Storms and Tornadoes: Observations and Dynamics*. Springer Berlin Heidelberg: Springer-Verlag. ISBN: 978-3-642-05380-1, 456 pp.

Brooks EM. 1951. Tornadoes and related phenomena. In *Compendium Meteorology*, Malone TF (ed). American Meteorological Society: Boston, MA, USA, 673–680.

Carapiperis LN. 1952. On the surface temperature of Greek waters. *Pure Appl. Geophys.* **23**(1): 153–161.

Doswell CA III, Schultz DM. 2006. On the use of indices and parameters in forecasting severe storms. *Electron. J. Severe Storms Meteorol.* **1**(3): 1–22.

Dotzek N, Groenemeijer P, Feuerstein B, Holzer MA. 2009. Overview of ESSL's severe convective storms research using the European Severe Weather Database ESWD. *Atmos. Res.* **93**: 575–586, doi: 10.1016/j.atmosres.2008.10.020.

Galway JG. 1956. The lifted index as a predictor of latent instability. *Bull. Am. Meteorol. Soc.* **37**: 528–529.

Gaya M. 2011. Tornadoes and severe storms in Spain. *Atmos. Res.* **100**(4): 334–343.

George JJ. 1960. *Weather Forecasting for Aeronautics*. Academic Press: London, UK, 673 pp.

Giaiotti DB, Giovannonni M, Pucillo A, Stel F. 2007. The climatology of tornadoes and waterspouts in Italy. *Atmos. Res.* **83**: 534–541.

Gianfreda F, Miglietta MM, Sans' o P. 2005. Tornadoes in Southern Apulia (Italy). *Nat. Hazards* **34**(1): 71–89.

Glickman TS (ed). 2000. *Glossary of Meteorology*, 2nd edn. American Meteorological Society: Boston, MA, 855 pp.

Golden JH. 1968. Waterspouts at Lower Matecumbe Key, Florida, 2 September 1967. *Weather* **23**: 103–114.

Golden JH. 1971. Waterspouts and tornadoes over south Florida. *Mon. Weather Rev.* **99**: 146–154.

Golden JH. 1973. Some statistical aspects of waterspout formation. *Weatherwise* **26**: 108–117.

Golden JH. 1974a. The life cycle of Florida Keys' waterspouts I. *J. Appl. Meteorol.* **13**: 676–692.

Golden JH. 1974b. Scale-interaction implications for the waterspout life cycle II. *J. Appl. Meteorol.* **13**: 693–709.

Golden JH. 1977. An assessment of waterspout frequencies along the U.S. east and Gulf states. *J. Appl. Meteorol.* **16**: 231–236.

Golden JH. 2003. Waterspouts. In *Encyclopedia of Atmospheric Sciences*, Holton JR (ed). Academic Press: Oxford, UK, 2510–2525, doi: 10.1016/B0-12-227090-8/00451-6. ISBN: 9780122270901.

Golden JH, Bluestein HB. 1993. The NOAA-National Geographic Society waterspout expedition. *Bull. Am. Meteorol. Soc.* **75**(12): 2281–2288.

Golden JH, Sabones ME. 1991. Tornadic waterspout formation near interesting boundaries. In *Preprints, 25th International Conference on Radar Meteorology*, Paris, American Meteorological Society, 420–423.

Groenemeijer P, Kühne T. 2014. A climatology of tornadoes in Europe: results from the European Severe Weather Database. *Mon. Weather Rev.* **142**(12): 4775–4790.

Hess GD, Spillane KT. 1990. Waterspouts in the Gulf of Carpentaria. *Aust. Meteorol. Mag.* **38**: 173–180.

Hurd WE. 1950. Some phases of waterspout behavior. *Weatherwise* **3**: 75–82.

Kamperakis NC, Nastos PT, Matsangouras IT. 2014. Using data mining methods in forecasting waterspouts over south Aegean Sea. In *14th EMS/10th ECAC Annual Meeting Abstracts*, Vol. 11. EMS2014-537-1, Prague, Czech Republic, 6–10 October 2014.

Keul AG, Sioutas MV, Szilagyi W. 2009. Prognosis of central-eastern Mediterranean waterspouts. *Atmos. Res.* **93**(1–3): 426–436.

Leverson VH, Sinclair PC, Golden JH. 1977. Waterspout wind, temperature and pressure structure deduced from aircraft measurements. *Mon. Weather Rev.* **105**: 725–733.

Markowski P, Richardson Y. 2010. *Mesoscale Meteorology in Midlatitudes by Paul*. Wiley-Blackwell: Chichester, UK. ISBN: 978–0470742136, 430 pp.

Matsangouras IT, Nastos PT. 2013. Historical records of tornadic activity over Greece. In *7th European Conferences on Severe Storms (ECSS2011)*, ECSS2013-236, Palma de Mallorca Balearic Islands, Spain, 3–7 June 2013.

Matsangouras IT, Nastos PT. 2014. An online reposting system for tornadoes, waterspouts and funnel clouds activity over Greece: http//tornado.geo.uoa.gr. In *10th International Congress of the Hellenic Geographical Society*, Thessaloniki, Greece, 22–24 October 2014.

Matsangouras IT, Nastos PT, Smith R, Blair D, Dahni R. 2013. An objective synoptic classification of tornadic days over Greece. In *13th Annual Meeting of the European Meteorological Society (EMS) and the 11th European Conference on Applied Climatology (ECAC)*,Vol. 29, EMS2013-514, Reading, UK, 9–13 September 2013.

Matsangouras IT, Nastos PT, Bluestein HB, Sioutas MV. 2014. A climatology of tornadic activity over Greece based on historical records. *Int. J. Climatol.* **34**: 2538–2555, doi: 10.1002/joc.3857.

Matsangouras IT, Nastos PT, Pytharoulis I. 2016. Study of the tornado event in Greece on March 25, 2009: synoptic analysis and numerical modeling using modified topography. *Atmos. Res.* **169**: 566–583, doi: 10.1016/j.atmosres.2015.08.010.

McCarthy DW. 2003. NWS tornado surveys and the impact on the national tornado database. First Symp. on F-Scale and Severe Weather Damage Assessment, Long Beach, CA, *Amer. Meteor. Soc.*, 3.2.

Metaxas DA, Bartzokas A. 1994. Pressure covariability over the Atlantic, Europe and N. Africa. Application: centers of action for temperature, winter precipitation and summer winds in Athens, Greece. *Theor. Appl. Climatol.* **49**: 9–18, doi: 10.1007/BF00866284.

Miglietta MM, Rotunno R. 2016. An EF3 multi-vortex tornado over the Ionian region: is it time for a dedicated warning system over Italy? *Bull. Am. Meteorol. Soc.* **97**: 23–30.

Miller RC. 1967. Notes on analysis and severe storm forecasting procedures of the Air Force Global Weather Central. Technical Report 200(Rev.), Air Weather Service, Scott Air Force Base, IL, 190 pp.

Miller RC, Bidner A, Maddox RA. 1971. The use of computer products in severe weather forecasting (the SWEAT index). In *Preprints, Seventh Conference on Severe Local Storms*, Kansas City, KS, American Meteorological Society, 1–6.

Moncrieff MW, Miller MJ. 1976. The dynamics and simulation of tropical cumulonimbus and squall lines. *Q. J. R. Meteorol. Soc.* **102**: 373–394.

Nastos PT, Matsangouras IT. 2010. Tornado activity in Greece within the 20th century. *Adv. Geosci.* **26**: 49–51, doi: 10.5194/adgeo-26-49-2010.

Nastos PT, Matsangouras IT. 2012. Composite mean and anomaly of synoptic conditions for tornadic days over north Ionian Sea (NW Greece). In *Advances in Meteorology, Climatology and Atmospheric Physics*, Helmis CG, Nastos PT (eds). Springer: Berlin and Heidelberg, Germany, 639–645, doi: 10.1007/978-3-642-29172-2_91.

Nastos PT, Matsangouras IT. 2014a. Analysis of synoptic conditions for tornadic days over western Greece. *Nat. Hazards Earth Syst. Sci.* **14**(9): 2409–2421.

Nastos PT, Matsangouras IT. 2014b. Seasonal analysis of composite mean and anomaly of synoptic conditions during waterspout days over north Cretan Sea, Greece. In *COMECAP 2014 Book of e-contributions. Proceedings 12th International Conference of Meteorology, Climatology and Physics of the Atmosphere*, Kanakidou M, Mihalopoulos N, Nastos P (eds). Herakleio, Greece, Crete University Press, 299–303.

Peterson GA. 1963. Funnel clouds in Hawaii. *Mon. Weather Rev.* **105**: 191–192.

Poulos SE, Drakopoulos P, Collins MB. 1997. Seasonal variability in the oceanographic conditions in the Aegean Sea (eastern Mediterranean): an overview. *J. Mar. Syst.* **3**(1–4): 225–244.

Price S, Sasaki RI. 1963. Some tornadoes, waterspouts, and other funnel clouds of Hawaii. *Mon. Weather Rev.* **91**: 175–192.

Rennó NO, Bluestein HB. 2001. A simple theory for waterspouts. *J. Atmos. Sci.* **58**(8): 927–993.

Rennó NO, Burkett ML, Larkin MP. 1998. A simple thermo dynamical theory for dust devils. *J. Atmos. Sci.* **55**: 3244–3252.

Schaefer J, Edwards P. 1999. The SPC tornado/severe thunderstorm database. Preprints, 11th Conf. on Applied Climatology, Dallas, TX, *Amer. Meteor. Soc.*, 603–606.

Schwiesow RL. 1981. Horizontal velocity structure in waterspouts. *J. Appl. Meteorol.* **20**: 349–360, doi: 10.1175/1520-0450(1981)020<0349:HVSIW>2.0.CO;2.

Showalter AK. 1947. A stability index for forecasting thunderstorms. *Bull. Amer. Meteor. Soc*. **34**: 250–252.

Simpson J, Morton BR, McCumber MC, Penc RC. 1986. Observations and mechanisms of GATE waterspouts. *J. Atmos. Sci.* **43**: 753–783, doi: 10.1175/1520-0469(1986)043<0753:OAMOGW>2.0.CO;2.

Sioutas MV. 2011. A tornado and waterspout climatology for Greece. *Atmos. Res.* **100**: 344–356.

Sioutas M, Szilagyi W, Keul A. 2013. Waterspout outbreaks over areas of Europe and North America: environment and predictability. *Atmos. Res.* **123**: 167–179.

Szilagyi W. 2009. A waterspout forecasting technique. In *5th European Conference on Severe Storm*s, ECSS-129, Landshut, Germany, 12–16 October 2009.

Wakimoto RM, Lew JK. 1993. Observations of a Florida waterspout during Cape. *Weather Forecast.* **8**(4): 412–423.

Weisman ML, Klemp JB. 1982. The dependence of numerically simulated convective storms on vertical wind shear and buoyancy. *Mon. Weather Rev.* **10**: 504–520.

Williams ER, Renno N. 1993. An analysis of the conditional instability of the tropical atmosphere. *Mon. Weather Rev.* **121**: 21–36.

Woodley WL, Golden JH, Halter BC. 1967. Aircraft observations in the immediate vicinity of two waterspouts. *Mon. Weather Rev.* **95**: 799–803.

